J Geod (2015) 89:519–536
DOI 10.1007/s00190-015-0795-3

ORIGINAL ARTICLE

GPS radio occultation constellation design with the optimal performance in Asia Pacific region

Milad Asgarimehr · Masoud Mashhadi Hossainali

Received: 5 July 2014 / Accepted: 10 February 2015 / Published online: 27 February 2015

Abstract The growing desire for better spatial and also temporal distribution of radio occultation data is a motivation for extensive researches considering either number of GNSS/receiver satellites or better optimization tools resulting in better distributions. This paper addresses the problem of designing a global positioning system-only radio occultation mission with the optimal performance in Asia Pacific region. Constellation Patterns are discussed and 2D-lattice and 3D-lattice flower constellations are adopted to develop a system with circular and elliptical orbits, respectively. A perturbed orbit propagation model leading to significantly more accurate pre-analysis is used. Emphasizing on the spatial and also temporal distribution of radio occultation events for the first time, distribution norm is provided as a volumetric distribution measure using Voronoi diagram concept in a 3D space consisting temporal and spatial intervals. Optimizations are performed using genetic algorithm to determine optimal constellation design parameters by the suitable fitness function and constraints devised. The resulted constellation has been evaluated by a regional comparison to the globally distributed FORMOSAT-3/COSMIC in terms of the distribution norm, number of radio occultation events and also coverage as an additional point-to-point distribution measure. Although it is demonstrated that the optimal 3D-lattice enjoys better performance than FORMOSAT-3, the design approach results in a 2D-lattice flower constellation which is superior to other constellations in regional emphasis of radio occultation events. Its global performance is discussed and it is demonstrated that using multi-GNSS receiver to increase satellites may not guarantee a good distribution of radio occultation data in some aspects.

Keywords Constellation design · Radio occultation mission · Genetic algorithms · Constellation patterns · Voronoi diagram · FORMOSAT-3/COSMIC

M. Asgarimehr (✉) · M. M. Hossainali
Department of Geodesy and Geomatics Engineering,
K. N.Toosi University of Technology,
No. 1346, Vali_Asr Ave., Mirdamad Cr., Tehran, Iran
e-mail: miladasgarimehr@gmail.com

M. M. Hossainali
e-mail: hossainali@kntu.ac.ir

1 Introduction

Ease of using satellite constellations for atmosphere monitoring and significant amount of data obtained through GPS radio occultation (RO) made a revolution in meteorology data acquisition techniques. A groundbreaking work to experience RO technique was made by Marine-IV in 1964 to measure Mars's atmosphere and ionosphere directly (Kliore et al. 1965). These very first valuable data led to emergence of missions planned to study atmosphere of planets and their moons (Yunck et al. 2000). Later, unknown planetary atmosphere was not the only motivation of using this technique. So, RO was introduced as an alternative method to study the Earth's atmosphere in the GPS/MET experiment (Bevis et al. 1994). Achievements of low Earth orbit (LEO) satellites and the global positioning system (GPS) cooperation in obtaining atmospheric and ionospheric density information using the inversion techniques, caused the idea to add RO as a sub mission to geodetic LEO missions such as GRACE and CHAMP (Wickert et al. 2009). Major weather centers and scientific communities have widely utilized these accurate and stable data for the atmospheric meteorology, ionosphere, and geodesy researches (Anthes 2011; Brunini et al. 2013; Le Marshall et al. 2012).

As meteorology models of weather and atmosphere are highly dependent on temporal and spatial distribution of pro-

vided data, a single spacecraft as a GNSS observer may fail to achieve the sufficient distribution. This fact is the motivation to design and deploy RO mission systems utilizing multiple satellites. FORMOSAT-3/COSMIC constellation consisting of six LEO satellites is the world's first operational GPS RO constellation. The data as received by FORMOSAT-3/COSMIC satellites have been processed in near real time into 2500 good ionospheric profiles and 1800 good atmospheric profiles per day (Fong et al. 2009). Following the achieved successes by FORMOSAT-3, another constellation consisting 12 satellites is planned to be launched in two stages entitled FORMOSAT-7/COSMIC-2. Six satellites will be launched to low-inclined orbits in 2016 while the others will be deployed in high-inclined orbits in 2018. The six satellites planned to be launched in low-inclined orbits will be utilized to improve the RO distribution in equatorial regions where Taiwan is located as one of the program responsible governments (Cook et al. 2013). This fact demonstrates the increasing desire for more well-distributed ROs in specific regions and can be a sign of regional optimized RO constellations development in near future. Also, FORMOSAT-7 is supposed to collect more RO data profiles using Galileo and GLONASS tracking capability which will produce a significantly higher spatial and temporal density of profiles than the systems tracking only GPS signals.

According to importance of distributions provided by these systems, obtaining the optimal performance of the system over the desired region is the key sector of designing and deploying of such systems. Better distribution will lead to better meteorological numerical models and products. In this regard, various researches have attempted to propose the constellations and design approaches leading to larger number of ROs distributed better. Hence, Mousa et al. (2006) proposed a simulation approach to determine the best practical orbital parameters of a LEO satellite for a tropical GPS RO mission based on number of ROs. Following success of satellite systems consisting multiple satellites, Walker constellations have been optimized using genetic algorithm (GA) by Juang et al. (2013) in order to address requirements of maximizing the regional spatial distribution of RO events while maintaining an acceptable uniform spatial distribution globally. This paper was a successful initial effort to optimize an RO constellation spatially by simply devising a fitness function based on the brute force grid search. Almost simultaneously, Lee and Mortari (2013) proposed an approach to optimize recently proposed 2D flower constellation for a LEO–LEO RO mission by optimizing this constellation by GA based on the odds at which pairs of satellites can see each other through the atmosphere (active or observation time). This creative approach resulted in a constellation with worthy characteristics which can be studied in the corresponding paper. Following further refinements to address determination of parameters defining a RO constellation, this research focuses on an approach to design a suitable geometry of LEO satellites to reach the desired regional performance for a GPS RO mission while a global coverage is a secondary mission objective. By a study on distribution concepts and with the help of Voronoi diagram, the fitness function is devised so that not only to meet the spatial distribution but also to improve the temporal distribution of ROs. The study area is Asia Pacific region consisting of the countries which are active members in Asia Pacific Space Cooperation Organization (APSCO). So, in this research, the term Asia Pacific refers to Asia and the Pacific region (not only the Pacific region of Asia). In this paper, alternative satellite constellations theorized as a framework for constellation designs are introduced in Sect. 2. Satellites' motion dynamics and orbits' propagation algorithm are described by Sect. 3 in a nutshell. After describing a radio occultation event (ROE) simulation by Sects. 4 and 5 discusses on the genetic algorithm (GA) and the adopted scheme. The devised fitness function, constraints and performance measures which are deployed for such mission evaluation are introduced in Sect. 6 to define the optimization problem clearly. After detailed description of numerical and evaluating results in Sect. 7, outlines are extracted in Sect. 8 as the conclusion.

2 Constellation patterns

A satellite orbit in space is specified with six continuous parameters known as Keplerian elements. With six orbital elements per satellite, the optimization problem may be intractable and also sometimes impractical. To make the problem solvable, the prominent constellation patterns are considered as a framework which is a strong constraint on the design space mathematically. This consideration not only minimizes the variables of optimization problems, but also helps achieve some prerequisites of the mission such as coverage symmetry and spacecraft collision avoidance in orbit intersections. Moreover, these patterns consider similar orbit properties such as height and inclination which lead to similar interactions of perturbation forces on motion dynamics of spacecraft. So, the symmetry lasts more without the usage of propulsion engines and the space segment maintenance costs are economized. In this section, these patterns are introduced briefly.

2.1 Streets of coverage

The first and leading approach to design a constellation typically involves multiple satellites which are placed on polar circular orbits at the same altitude to create streets of coverage such that the ground coverage of satellites in adjacent planes overlaps provides a full coverage scheme. In each orbital plane there are q satellites evenly spaced.

The n polar orbital planes are evenly distributed within 180° on the equator (Rider 1985, 1986). This constellation represents the simplest method to reach a global coverage and may be appropriate for a communication mission, while the polar caps enjoy more coverage than the equatorial regions. This property is obviously a disadvantage of such constellations.

2.2 Walker constellation

The second constellation which is more popular and used in different missions is Walker constellation (Walker 1977, 1978). Walker consists of T satellites evenly distributed in P orbit planes. So each orbital plane contains S satellites. All of the orbit planes are assumed to be at the same inclination, i, relative to the equator. The ascending nodes of the P orbit planes are uniformly distributed around the equator (i.e., at intervals of $360/P$). Also, the S satellites are uniformly distributed within each orbital plane (i.e., at intervals of $360/S$). The integer value F, is the phase parameter that defines the spacing between spacecrafts in adjacent orbital planes by $\Delta\varphi = 360F/T$, where $\Delta\varphi$ is the phase difference between spacecraft in adjacent orbital planes. Range of F is $0 < F < P - 1$.

2.3 Flower constellations

To place all satellites on the same closed trajectory in a rotating reference frame, e.g., Earth-Centered Earth-Fixed (ECEF), flower constellations (FCs) were proposed (Mortari et al. 2003). A FC consists of N_s satellites with the period T_p which is a rational multiple of the period of rotating frame, T_d. It can be written as:

$$N_p T_p = N_d T_d \tag{1}$$

where N_p and N_d are some positive coprime integers. While the semi-major axis, a, eccentricity, e, inclination, i, and argument of perigee, ω, are chosen identical for all of the satellite orbits, The mean anomaly, M_k, and the right ascension of the ascending node (RAAN), Ω_k, of each satellite ($k = 1, \ldots, N_s$) satisfy (Mortari and Wilkins 2008; Wilkins and Mortari 2008):

$$N_p \Omega_k + N_d M_k = \text{const} \bmod (2\pi) \tag{2}$$

Despite the symmetry consideration in designing a Walker constellation, there is no necessity to reach a symmetric geometry of spacecrafts in initial proposed theory of FCs while it is possible to obtain a subset of FCs characterized by symmetric distributions, so-called harmonic flower constellations (HFCs).

2.3.1 The 2D lattice flower constellation

Using the initial theory of FCs to achieve the optimized HFCs may be quite complicated and computationally intensive, while the 2D lattice flower constellation (2D-LFC) is the minimum-parameter description of HFCs (Avendaño et al. 2013).

The 2D-LFCs are defined by five integer parameters $\{N_o, N_{so}, N_c, N_p, N_d\}$ and three continuous parameters $\{a, e, i\}$. While most of these parameters are already introduced, new parameters N_o, N_{so} and N_c represent the number of orbital planes, number of satellites per orbit and a phasing parameter, respectively. Unlike the original definition of FCs, usage of N_p and N_d satisfying the compatibility Eq. (1) is optional since repeating ground-track requirement is not enforced in general 2D-LFC framework. In a 2D-LFC RAAN and initial mean, anomaly is defined as (Avendaño et al. 2013):

$$\begin{bmatrix} N_O & 0 \\ N_c & N_{SO} \end{bmatrix} \begin{bmatrix} \Omega_{ij} \\ M_{ij} \end{bmatrix} = 2\pi \begin{bmatrix} i-1 \\ j-1 \end{bmatrix} \tag{3}$$

where $i = 1, \ldots, N_o$, $j = 1, \ldots, N_{so}$, and $N_c \in [1, N_{so}]$. Satellite (i, j) is the j-th satellite on the i-th orbital plane.

Even though using elliptical orbits in a 2D-LFC framework leads to uniform and symmetric constellations, the uniformity and the symmetry will be destroyed by Earth's oblateness (J_2) effect as the most important perturbation of LEO satellites. Hence, the circular orbits are adopted for a 2D-LFC in practice while another framework which maintains the symmetry for elliptical orbits is proposed and introduced in Sect. 2.3.2.

It should be noted that when circular orbits are used, Walker constellation can be regarded as a 2D-LFC and also any LFC can be obtained as a Walker constellation. For details, see Avendaño et al. (2013).

2.3.2 The 3D lattice flower constellation

Given the disadvantage of 2D-LFCs in using elliptical orbits, The 3D lattice flower constellations (3D-LFC) were developed as a framework yielding the symmetry and the needed spacing even in utilizing elliptical orbits (Davis et al. 2013).

In 3D-LFC notation, we use N_ω and N'_{so} to represent number of unique orbits (with different arguments of perigee) on each plane and the number of satellites on each of those orbits, respectively. Simply, number of satellites is $N_S = N_O N_\omega N'_{SO}$.

Here, three parameters are used as phasing parameters which are N_c^1, N_c^2 and N_c^3 to do the spacing of satellites by:

$$\begin{bmatrix} N_o & 0 & 0 \\ N_c^3 & N_\omega & 0 \\ N_c^1 & N_c^2 & N'_{so} \end{bmatrix} \begin{bmatrix} \Omega_{ijk} \\ \omega_{ijk} \\ M_{ijk} \end{bmatrix} = 2\pi \begin{bmatrix} i-1 \\ k-1 \\ j-1 \end{bmatrix} \tag{4}$$

where $i = 1, \ldots, N_o$, $j = 1, \ldots, N'_{so}$, $k = 1, \ldots, N_\omega$, and $N_c^1 \in [1, N_o]$, $N_c^2 \in [1, N_\omega]$, and $N_c^3 \in [1, N_o]$. Also, satellite (i, j, k) is the i-th satellite on the j-th orbital plane and k-th unique orbit of this orbital plane. See Davis et al. (2013) for details.

3 Satellite spacecraft dynamics and orbits' simulation

Orbit propagation can be the key sector of pre-analysis of a constellation design. Due to complicated dynamics of spacecraft in space, there are always simplifications in the simulation. The level of this simplification strongly depends on the requirements and the mission objectives. Oversimplified models can lead to an unexpected inaccuracy in the constellation pre-analysis which may result in the mission failure. In this section, it is attempted to have a general overview on satellites motion in space and methods to model and simulate an orbit.

Keplerian motion or the two-body problem is the most simplified motion of satellites which supposes the motion environment as a central force field. According to Newton's second law of motion, simply we can show that the following equation governs the satellites' motion (Xu 2008, pp. 27–29):

$$\ddot{\vec{r}} = -\frac{\mu}{r^3}\vec{r} \tag{5}$$

in which μ is the planetary gravitational constant, $\vec{r}$ and $\ddot{\vec{r}}$ are the position vector of the satellite relative to the center of the Earth and its second-order derivate, respectively. The three Keplerian laws, published by Johannes Kepler (1571–1630) in the span of several years, derived using Tycho Brahe's observations of Mars, can be mathematically proven by Eq. (5). For Keplerian laws and the proofs see (Seeber 2003, pp. 62–81).

By considering $\vec{r}_0$ and $\dot{\vec{r}}_0$, the position and velocity of a satellite at the initial time, this second-order, nonlinear differential equation is solved as an initial value problem (IVP) in an inertial framework (since the Newton's second law is only valid in an inertial framework), such as the most commonly used reference frame, the Earth-centered inertial (ECI). As the next step, another reference frame should be defined where the geographical coordinates of points on the Earth do not change in and the coordinates are transformed to, such as ECEF. The geometric properties of orbit and the Keplerian elements can be extracted from the state vector, $\vec{S} = \left[\vec{r}\ \dot{\vec{r}}\right]$ which can be determined at the desired time spans (Xu 2008, pp. 27–38). Computing the spacecraft trajectory for a desired period of time in Keplerian motion can be so easier using the Keplerian propagation algorithms.

A perturbation is a deviation from Keplerian motion. The actual path will vary from the theoretical two-body problem since the spacecraft is not governed by only a central force field. This motion is affected by perturbation forces such as non-spherical Earth's gravitational field, Sun's and the Moon's gravitations, Earth tide and ocean tide loading, solar radiation pressure and atmospheric drag. The acceleration due to each perturbation force can be modeled and computed, however, the acceleration resulted by some of these forces cannot be obtained easily. Refer to Xu (2008, pp. 46–66) for a complete survey of modeling perturbation accelerations. So, as a perturbed equation of motion, Eq. (5) can be rewritten as follows:

$$\ddot{\vec{r}} = -\frac{\mu}{r^3}\vec{r} + \vec{a}_p \tag{6}$$

where $\vec{a}_p$ is the resultant acceleration of perturbation forces. Since the precisely analytic resolution of this equation is not possible, numerical integration and interpolation algorithms are suggested (Xu 2008, pp. 178–189). The state vector is computed at mesh points and position and velocity of spacecraft are extracted throughout the needed time span. Figure 1 displays the perturbed propagation algorithm.

4 Radio occultation event simulation

Global positioning system (GPS) radio occultation (RO) is a term used for a remote sensing technique. What this technique needs is an observation of a GPS satellite's (or any other GNSS satellites') signal which passes through atmosphere of the study planet (usually the Earth). The atmospheric properties are extracted through the detection of a change in the observed radio signal due to electromagnetic radiation refraction during its pass through the atmosphere. The prerequisite for such event is a specific relative geometry of the receiver satellite (LEO satellite) and GPS one. So, if the sight line of satellites passes through the Earth's atmosphere, it can be considered as an ROE. Then, the only parameter needed to be obtained is the elevation of the sight line relative to Earth's surface. To this end, using position vectors of LEO and GNSS satellite in ECI framework represented by $\vec{r}_{\text{LEO}}$ and $\vec{r}_{\text{GNSS}}$ as well as $\vec{r}_{\text{LOS}}$ as the line of sight vector, $\vec{R}$, a vector which is perpendicular to $\vec{r}_{\text{LOS}}$ and its origin is at the center of the Earth must be determined. According to the cosine rule, we can write:

$$\alpha = \cos^{-1}\left(\frac{r_{\text{LOS}}^2 + r_{\text{LEO}}^2 - r_{\text{GNSS}}^2}{2 r_{\text{LEO}} r_{\text{GNSS}}}\right) \tag{7}$$

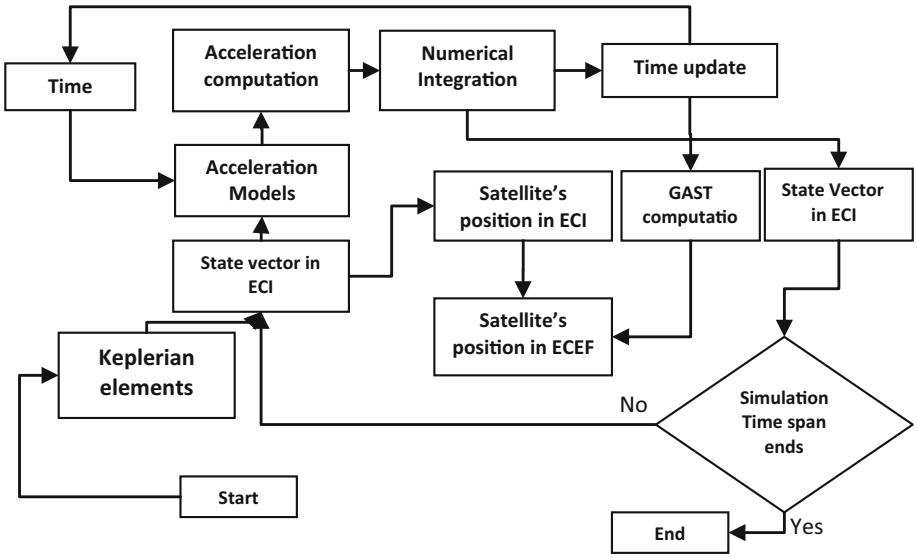

Fig. 1 Purturbed orbit propagation algorithm

where $r = \text{norm}(\vec{r})$ and α is the angle between $\vec{r}_{\text{LOS}}$ and $\vec{r}_{\text{LEO}}$ whose origin is on the LEO satellite. Easily we can write:

$$\vec{R} = \vec{r}_{\text{LEO}} + r_{\text{LEO}} \cos(\alpha)\vec{e}_{r\text{LOS}} \tag{8}$$

where $\vec{e}_{r\text{LOS}} = \vec{r}_{\text{LOS}}/r_{\text{LOS}}$. Simply if norm($\vec{\text{R}}$) is between the atmosphere height and the Earth's radius, the geometry satisfies the radio occultation event. Normally, the Earth is considered as a perfect sphere for this purpose. Here, the flattening of the Earth has been taken into account. To take into account the elliptical shape of the Earth, $\vec{R}$ is transformed from ECI to ECEF coordinates and then from ECEF to the system of geodetic coordinates. Indicating $\vec{R}$ in a geodetic system helps compute its height in a geodetic global reference frame comprising a standard coordinate system for the Earth and a standard spheroidal reference surface (the datum) for the altitude data. The World Geodetic System 84 (WGS-84) is used in this research.

Then, using propagation models, GPS and the proposed constellation satellites' coordinates are determined in an interval of 10 s. In each epoch, radio occultation occurrence is checked by computing $\vec{R}$ for the all possible pairs of LEO and GPS satellites. So, if the geodetic height of $\vec{R}$ is a value between the atmosphere height (100 km) and zero, the event will be recorded as a ROE.

5 Deployment of genetic algorithm

GA has been introduced as a robust technique to solve many multivariable problems (Fonseca and Fleming 1993; Goldberg and Holland 1988). Optimum satellite constellation has been resolved for various missions based on different criteria by GA (Abdelkhalik and Gad 2011; Asvial et al. 2004; Crossley and Williams 2000; Ely et al. 1999; Yan et al. 2013). In this research, GA is applied to obtain the constellation parameters. GA is an optimization technique which is based on searching in the solution space to find an optimal solution or the one which possesses the desired qualifications. GA imitates natural biological evolution based on 'survival of the best' rule. In this technique, each solution in the search space is represented by a chromosome which is typically a binary encoded string. A set of chromosomes makes up a population and the first population is generally generated randomly. The evolutionary process uses successive iterations of selection, crossover and mutation. By the act of these genetic operators, a new population with the same number of chromosomes is reproduced to improve the quality of the candidate solutions represented as the population. So, a fitness function must be devised helping the selection from the current population based on fitness modified through crossover and mutation operations to form a new population (Goldberg and Holland 1988). The new population is used as next generation and this trend will continue until the stop condition is established. The stop condition can be a maximum number of generations reached, a satisfactory fitness level achievement for the population or reach a certain threshold number for successive iterations without any improvement in the fitness value.

In this research, each optimization parameter (described in Sect. 6.3.2) is represented by 8 bits. 16 candidates are collected randomly as the initial population. After calculating the fitness value for each individual of the population by the defined fitness function (introduced in Sect. 6.1), the roulette wheel approach is considered as the scheme to choose individuals for birth according to their fitness values. Then, one-point crossover approach is applied to generate the new population (Poli and Langdon 1998). It should be noted that the mutation is also carried out at a rate of 0.15. After that, the new population will be inputted into the next iteration until

the stop condition is met which is 10 successive iterations without any improvement in fitness value of the best solution (best candidate of the population).

6 Fitness function and evaluation criteria

In GA, the fitness function has the most important role since it leads the optimization process to the parameters which satisfy the mission objectives. The temporal and spatial distribution of radio occultation events are as important as number of radio occultation events. In other words, these observations must cover the area spatially as well as temporally to have monitoring samples of the atmosphere throughout the desired region and time span.

Mathematically, point distributions on a space need to have the three attributes below to support the requirements mentioned above (Gunzburger and Burkardt 2004):

1. The points are equally spaced.
2. The points cover the region, i.e., there do not exist relatively large sub-regions that contain no points.
3. The points are isotropically distributed, i.e., there is no directional bias in the placement of points.

6.1 Distribution norm

Based on the three above properties, to achieve a constellation with a suitable performance, the concept of Voronoi diagram is deployed (Aurenhammer 1991). Voronoi diagram is a technique to divide the space into a number of regions (cells). For this purpose, a set of points, so-called generators, is already specified. For each generator, a corresponding region is defined consisting of all points of space closer to that generator than to any other. Mathematically, consider that X is a non-empty set representing a space whose distance function is d. If N generators are specified in X, $(P_k)_{k\in K}$, $K = \{1, \ldots, N\}$, is a non-empty subset of X which represents the generators. V_k is a subset of X whose distance to the generator P_k is not larger to any other P_j, $j \neq k$ and $j \in K$. Denoting the distance between two points x and a by $d(x, A) = \inf\{d(x, a) \mid a \in A\}$, we can write:

$$V_k = \{x \in X \mid d(x, P_k) \leq d(x, P_j) \quad \text{for all } j \neq k\} \tag{9}$$

A Voronoi tessellation is then defined as $v = \{P_k, V_k\}_{k=1}^{N}$. Given the N occultation data $\{z_i\}_{i=1}^{N}$ provided in space (Ω_{ROE}) introduced in Sect. 6.2, the Voronoi tessellation is $v_{ROE} = \{z_i, V_i\}_{i=1}^{N}$.

Using a volumetric uniformly measure, the fitness value of GA is defined as the point distribution norm, h, given by (Gunzburger and Burkardt 2004):

$$h = \max(h_i) \tag{10}$$

where:

$$h_i = \max d(z_i, y) \tag{11}$$

where $i = 1, \ldots, N$ and also $y \in V_i$.

This measure provides a good insight into how close a radio occultation event distribution is to an ideal uniform distribution and how far the maximal distance between any points in the space is to the nearest radio occultation event. The smaller the value of h, the better performance of the RO mission. Hence, GA is carried out to optimize distribution norm of 24-h ROEs provided by the constellation.

6.2 Measure space

Since the temporal distribution is as important as the spatial one, time as an additional dimension of space is also taken into account, i.e., $\Omega_{\mathrm{ROE}} \equiv (\varphi_{\mathrm{ROE}}, \lambda_{\mathrm{ROE}}, t_{\mathrm{ROE}})$ where $5°\mathrm{N} \leq \varphi_{\mathrm{ROE}} \leq 53°\mathrm{N}$, $25°\mathrm{E} \leq \lambda_{\mathrm{ROE}} \leq 135°\mathrm{E}$ (the Asia Pacific region) and $0\,\mathrm{h} \leq t_{\mathrm{ROE}} \leq 24\,\mathrm{h}$ are the latitude, longitude and time of ROEs. To adopt simultaneous use of temporal and spatial concepts in a 3D coordinate system, a compatible time parameter is made. To evaluate the performance of a mission, event times (t_{ROE}) are multiplied in the standardization parameter $G = D_{\max}/T_{\max}$ where $D_{\max}$ and $T_{\max}$ are the maximal possible distance in this region and the maximal possible time interval between two ROEs (i.e., 24 h). By application of this parameter, the temporal distribution is considered as important as the spatial one. However, multiplying G by a weight parameter k such that $k > 1$, the importance of temporal distribution is increased whereas when $0 < k < 1$ the value of the temporal distribution is decreased. So, all the distribution measures in this research consider points in a 3D space representing the distance including also temporal intervals by the scheme described here.

6.3 Constraints

In this research, these constraints are applied to the optimization problem; First, the suitable constellation pattern must be selected to determine the design parameters. Then, the design parameter constraints or their corresponding ranges must be defined to run the optimization process. As the last step of defining the constraints, the required prerequisites of the constellation must be introduced to GA mathematically.

6.3.1 Constellation pattern adoption

As seen before in Sect. 2, all the patterns can be regarded as the frameworks. But the suitability of the patterns must be discussed before optimization.

The radio occultation event always happens in a location between the GNSS' and the receiver satellite. Since locations of ROEs normally happen near to the receiver satellites' ground tracks, the optimal constellation is expected to provide orbit inclinations which do not exceed the maximum latitude of the area of interest. In other words, the constellation must be designed so that the satellites spend a major part of their revolution time over or near the region as much as possible. Such implementation of satellites cannot be met by streets of coverage provided by polar orbits. On the other hand, this constellation suffers from poor performance in equatorial regions and inhomogeneous coverage varying on different geographical latitudes. Due to such properties, it will not be used in the design process.

Walker constellation is well known due to the suitable symmetry provided. This constellation is flexible to be designed for different regions located in different latitudinal ranges. 2D-LFC possesses the same properties as Walker. This implies that the both constellations can be investigated for a radio occultation mission over Asia Pacific region. But as mentioned in Sect. 2.3.1, Walker constellation can be regarded as a 2D-LFC and also any 2D-LFC can be obtained as a Walker constellation if circular orbits are used. Since symmetric constellations provide better distributions of ROEs, circular orbits are used when the framework is 2D-LFC. Consequently, the 2D-LFC is considered as the framework of this research. Nevertheless, there is no need to investigate Walker constellations.

To date, there is no occultation mission deploying elliptical orbits. This might be due to the impacts of non-zero eccentricities such as additional orbit maintenance, non-constant altitude of the spacecrafts and thereby, the signal strength destabilization. The issue seems not to be addressed in previous researches as well. Nevertheless, the study can provide additional insights into the probable advantages or disadvantages of this type of orbits. To address this problem, elliptical orbits are optimized by considering 3D-LFC as the constellation in this research.

6.3.2 Design parameter constraints

Inclination (i), eccentricity (e) and phasing parameters (N_o, N_{so} and N_c for 2D-LFC and also N_o, N_ω, N_{so}, N_c^1, N_c^2, N_c^3 for 3D-LFC) are defined in specified ranges except the semi-major axis (a). Discussing on circular orbits, the lowest altitude which a spacecraft can orbit by 300 km due to atmospheric drag (i.e., $a_{\min} = R_e + 300$ km where R_e is Earth's radius). On the other hand, the Earth is surrounded by Van Allen belts. Van Allen belts refer to toroidal regions of charged particles: the altitude of the first ranges from 1000 to 10,000 km and the second from 13,000 to 65,000 km. The electronics of the spacecraft passing a long time through these regions are threatened by radiation. Hence, the maximum altitude of a LEO spacecraft can be 1000 km (i.e., $a_{\max} = R_e + 1000\,\text{km}$). In the case of elliptical orbits, the maximum altitude of apogee is set to 1000 km as well as minimum altitude of perigee considered 300 km. Hence, by a considered eccentricity, we have $a_{\min} = (R_e + 300\,\text{km})/(1-e)$ and also $a_{\max} = (R_e + 1000\,\text{km})/(1+e)$. It must be noted that the minimum eccentricity that the 3D-LFC can take for the orbits is $e_{\min} = 0.01$ to search just through the elliptical orbits and the maximum value of this parameter is 0.05 due to altitude limitations described above.

Considering 2D-LFC and 3D-LFC as the frameworks, two optimization processes should be run separately. The Asia Pacific GPS RO constellation is supposed to deploy six satellites. Accordingly, the design parameters of 2D-LFC and 3D-LFC and their ranges are defined and represented in Tables 1 and 2, respectively.

In this optimization problem, i, a and e are real-valued continuous variables. These variables are linearly mapped to a value in the corresponding specified range by 8 bits with an accuracy of three decimal places. The correlated parameters ($[N_o, N_{so}]$ in Table 1 and $[N_o, N_\omega, N'_{so}]$ in Table 2) need to be collected from one of the states represented in the tables. So, one parameter is specified to represent each state. The range of this parameter is specified according to number of states and the mapping accuracy. For $[N_o, N_{so}]$, the range is [0, 0.004] and also for $[N_o, N_\omega, N'_{so}]$ this range is specified as [0, 0.009]. Then each value corresponds to one state. Other integer parameters are mapped with a similar approach. These parameters must be collected in the specified ranges. Considering the mapping accuracy, these parameters are first

Table 1 Parameters range of 2D-LFC

Design parameter	Range
i	[1°, 180°]
a	$[R_e + 300\,\text{km}, R_e + 1000\,\text{km}]$
$[N_o, N_{so}]$	[1, 6], [2, 3], [3, 2], [6, 1]
N_c	$[1, N_o]$

Table 2 Parameters range of 3D-LFC

Design parameter	Range
i	[1°, 180°]
e	[0.01, 0.05]
a	$[\frac{R_e+300\,\text{km}}{1-e}, \frac{R_e+1000\,\text{km}}{1+e}]$
$[N_o, N_\omega, N'_{so}]$	[6, 1, 1], [3, 1, 2], [3, 2, 1], [2, 3, 1], [2, 1, 3]
	[1, 6, 1], [1, 1, 6], [1, 2, 3], [1, 3, 2]
N_c^1	$[1, N_o]$
N_c^2	$[1, N_\omega]$
N_c^3	$[1, N_o]$

mapped to a range 1000 times smaller. Then the value is multiplied by 1000 to reach an integer value in the desired range. (For example in Table 1, if $N_o = 6$, first the 8 bits are mapped to a value in [0, 0.006]. Then the value is multiplied by 1000 to reach an integer value in [0, 6]).

6.3.3 Collision and contact conflict avoidance

To avoid collision of the satellites, the minimum distance of the satellites ($\rho_{\min}$) for circular orbits can be determined by Speckman et al. (1990):

$$\rho_{\min} = 2a \left| \sqrt{\frac{1 + \cos^2 i + \sin^2 i \cos \Delta\Omega}{2}} \sin\left(\frac{\Delta F}{2}\right) \right| \quad (12)$$

where

$$\Delta F = \Delta M - 2 \tan^{-1}\left(-\cos i \tan\left(\frac{\Delta\Omega}{2}\right)\right) \quad (13)$$

In these equations, $\Delta\Omega$ and ΔM denote the difference in mean anomaly and right ascension of ascending node, respectively. Clearly, a zero distance implies the collision of satellites. But in this research, the smallest value that $\rho_{\min}$ can adopt is determined through ground contact considerations.

In developing a satellite system, each phase such as constellation, spacecraft and the ground system designs may interrelate. Design of the spacecraft and the ground system is out of the scope of this research. Therefore, the development phase aspects which might impose some restrictions on the constellation design are only pointed out here. Number of ground station and their locations are designed based on satellites coverage and data user needs while the balance against cost, accessibility and available communications is considered. The ground station design may affect the constellation design if some limitations exist in dedicated locations and software implementation. For example, orbits' inclination must be constrained if establishing a ground station in some areas is not possible (e.g., due to political issues). The semi-major axis is constrained when the satellites must have a repeating ground track due to a required pass over a specific station. Also, there are limitations in orbit altitude when the ground hardware cannot support some information transition rates. So, altitude and pass duration of the satellites must be adapted considering the hardware available at the ground stations. But, one of most important facts which can be addressed in the scope of this paper is the ground contact avoidance. According to constellation deployment for FORMOSAT-3/COSMIC mission, if there are two satellites flying over the same ground station at the same time frame, the ground station could support only one satellite (Fong et al. 2008). So contact conflict avoidance must be adopted as the additional constraint. In this regard, it is sufficient to guarantee that there is no pair of satellites whose footprints overlap at the same time. Hence, considering the satellites can be tracked from an elevation angle of 15°–15°, the minimum distance of any pair of satellites must be larger than twice the radius of satellites' footprints:

$$\rho_{\min} \geq 2(a - R_e) \cot 15^\circ \quad (14)$$

Although Eq. 12 only applies to circular orbits, similar computations can be made for constellations of elliptic orbits. This equation is also used to address the approach distance of apogees and perigees providing an insight into the collision avoidance (Davis et al. 2013). Moreover, According to Kessler (1990), orbiting in circular orbits is a common assumption to address collision avoidance since the calculation is easier and the most orbiting objects are in near circular orbits (especially in this research which the maximum eccentricity is considered 0.05 in). Since circular orbits spend all of their time at a particular altitude, their contribution to the collision probability is much higher than an elliptical orbit passing through the same altitude (Kessler 1990). The devised constraint is hence applied to elliptical orbit disregarding altitude changes' effects on the satellites footprints while the average altitude is used. The collision and contact conflict avoidance are applied by the penalty method. This method transforms the constrained problem to unconstrained one. If the constellations does not satisfy Eq. (14), the penalty term, $p = (D_{\max} + T_{\max})^{1/2}$, will be added to the fitness value.

Based on the preliminary studies on the suitability of the elliptical orbits in 3D-LFC, the optimization of the constellation irrespective of constraints on collision and contact conflict avoidance fails utterly, while the application of these constraints causes better convergence of GA to the optimal solution. These constraints not only provide a necessary prerequisite of the mission development but also yield better distribution of satellites such that a minimum distance is met.

6.4 Coverage

The devised fitness function enforces GA to search a solution which minimizes the maximal distance between any points of the space to the position of a ROE temporally and spatially during a day. It is expected that the distribution norm decreases as the number of ROEs increases since the measure depends on the number of ROEs. Nevertheless, distribution norm does not provide any insight into the point-to-point distribution of ROEs. For this purpose, another distribution measure is used. For any set of points $\{z_i\}_{i=1}^{N}$,

$$\lambda = \frac{1}{\bar{\gamma}} \left(\frac{1}{N} \sum_{i=1}^{N} (\gamma_i - \overline{\gamma})^2 \right)^{1/2} \quad (15)$$

where:

$$\gamma_i = \min_{j \neq i} d(z_i - z_j) \quad (16)$$

and:

$$\bar{\gamma} = \frac{1}{N} \sum_{i=1}^{N} \gamma_i \quad (17)$$

λ provides a measure which is dependent on the point-to-point distribution of ROEs. The measure λ is referred to coverage (COV) (Gunzburger and Burkardt 2004); the smaller value of λ is, the more uniform is the mesh. Unlike the distribution norm, λ is a measure which provides an insight to the point-to-point distribution of ROEs. This distribution measure does not depend on the number of ROEs and the volume of space.

7 Numerical results and evaluations

Using already discussed concepts, the numerical analysis and the optimization and evaluation processes are as follows:

7.1 Orbit propagation

In this research, orbits are modeled in three simplified approaches. The first propagated orbits are simulated Keplerian ones. The second propagation model enjoys a fourth-order gravitation field instead of a radial one. In the third propagation model, the atmospheric drag is also taken into account. The atmosphere density information is extracted from 1976 US standard atmosphere (Coesa 1976). Cook (1965) suggests the value of 2.2 for the atmospheric drag coefficient of compact satellites. To validate the propagation algorithm, the (real) orbit of the GRACE-1, as a LEO satellite, is compared to the simulated ones. This comparison is carried out on 1 November 2012 for 24 h. The corresponding circular position errors are represented as functions of time in Fig. 2.

It is found that in all cases, the difference between the GRACE real positions and the simulated orbits (i.e., the simulation error) oscillates with a period of approximately 50 min. The oscillation amplitude of 270 km is observed but it decreases during the time. The most important part is the secular errors increasing differently. The secular errors increase by 230, 70 and 40 km per 3 h for the Keplerian model, the fourth-order gravitation field, and the model including the atmospheric drag too, respectively. Based on the observed

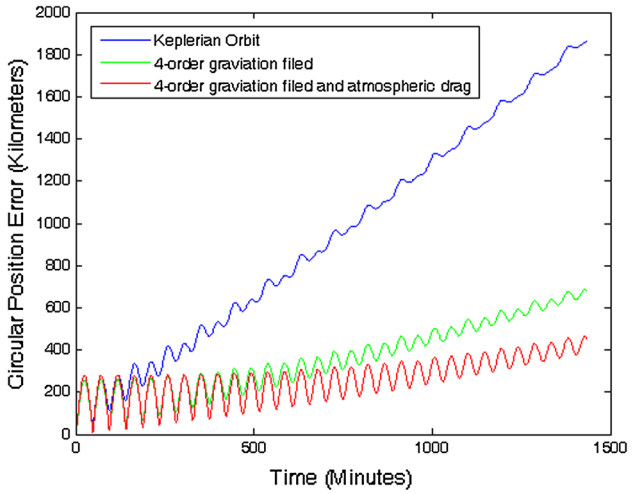

Fig. 2 The circular errors of the simulated orbits of GRACE-1 on 1 November 2012

results, simulated Keplerian model loses its accuracy after a while. This fact rejects the application of Keplerian models in LEO constellation design. It should be noted that although the precise computation of atmospheric drag is difficult and sometimes impossible, the third model approximates this perturbation so that the secular error reduces significantly. Although, the second model may be accurate enough to propose and evaluate a RO mission, the reduction of secular error is worthy enough to use the third model; however, this would be at the cost of more computation time. In this research, the fourth-order gravitational field and the atmospheric drag are modeled to propagate satellites orbits.

The effect of propagation errors on radio occultation events is also investigated through the simulation of a GPS ROEs for GRACE-1 on the same day. Figure 3 and Table 3 compare the ROEs for a simulated orbit of GRACE as well as its real positions extracted from LeoOrb files consisting precise LEO spacecraft orbits.

The ROEs locations are displayed in Fig. 3 for the simulated orbit (a) and the real one (b), for 24 h.

Given to Fig. 3 and Table 3, the simulation is sufficiently adequate for a quantitative 24-h analysis of observable radio occultation events.

This modeled is used to propagate the LEO satellites (i.e., satellites of the proposed constellation) and also satellites of the only considered GNSS (i.e., GPS) in the optimization process. It should be noted that the initial values (Keplerian elements) to solve Eq. 6 to propagate GPS orbits are extracted from Yuma almanacs in each day.

7.2 Optimum constellations

During optimization, any ROE with duration of <30 s is ignored since these ROEs are not probable to be recorded

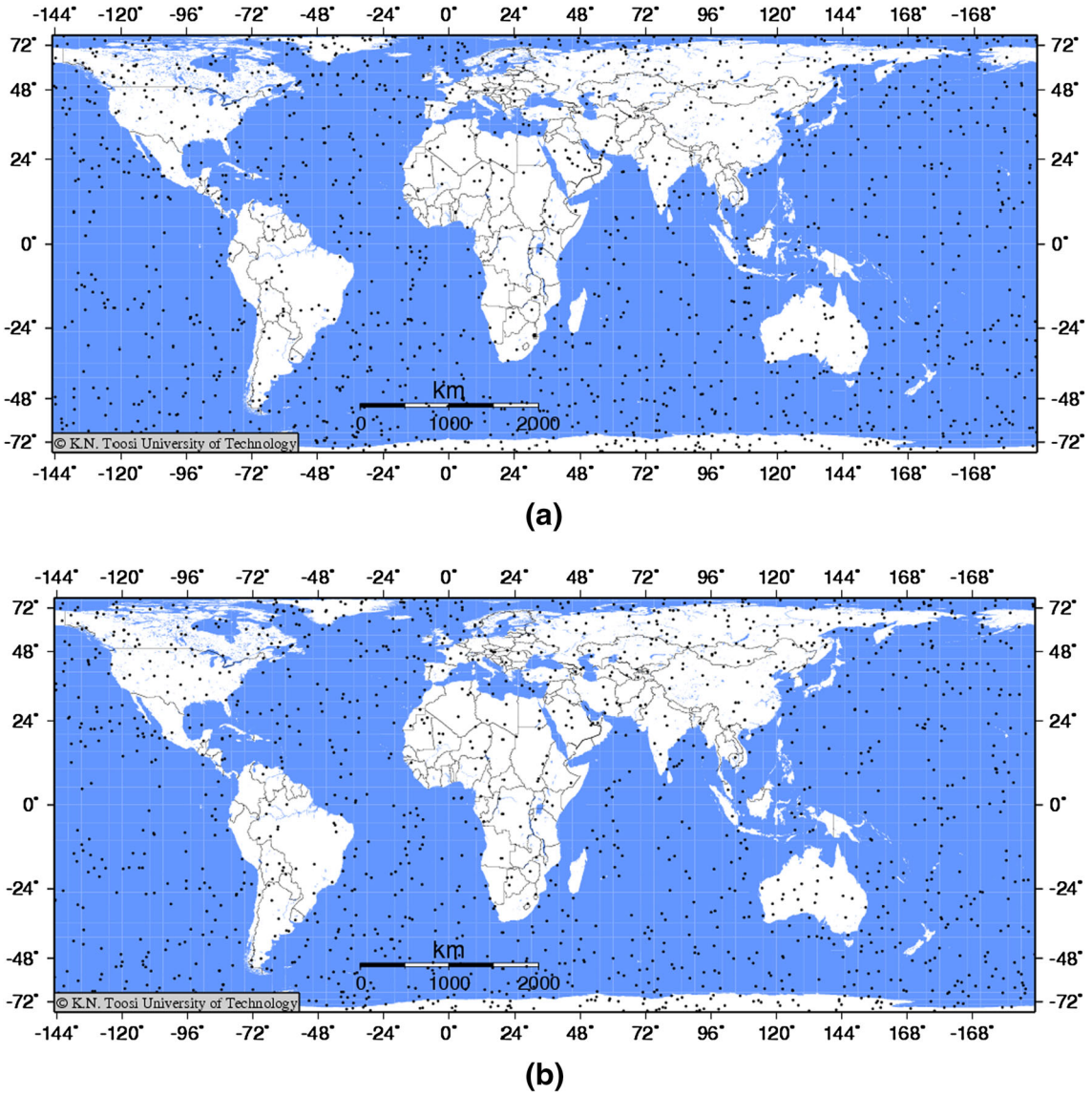

Fig. 3 Provided GPS ROEs of GRACE for the simulated orbit (**a**) and the real orbit (**b**) on 1 November 2012 for 24 h

Table 3 Simulation errors of evaluation measures

Measure orbit	Total number of ROEs	Number of ROEs in Asia Pacific region	The point distribution norm (h) in the region ($m \times 10^6$)	The COV measure (λ) in the region
Simulated orbit	1446	136	8.302	0.52
The real orbit	1441	134	8.618	0.56
Relative error	0.003	0.014	0.036	0.071

in a real environment due to the receivers' observation rate, antennas' field of view and signal blocking by the Earth's topography. Tables 4 and 5 report on the obtained parameters.

7.3 Regional performance evaluation

The GPS ROEs have been simulated for the performance analysis of the proposed constellations. GPS orbital period

Table 4 The parameters defining the optimal 2D-LFC

a (km)	i (°)	e	N_o	N_{so}	N_c
6877.555	38.235	0	3	2	2

Table 5 the parameters defining the optimal 3D-LFC

a (km)	i (°)	e	N_o	N_ω	N'_{so}	N_c^1	N_c^2	N_c^3
6964.941	50.053	0.02	2	3	1	2	2	1

is 11 h: 58 min, and as a result, it takes about one whole year for the GPS satellites to appear again in the same position at the exact time. Since repeating the analysis for the whole year is troublesome and impractical, the simulation was carried out for the first day of each month in 2013. This performance is compared to the existing global RO mission, the FORMOSAT-3/COSMIC, since there is no mission developed regionally in Asia Pacific region. This mission orbits by altitude of 750–800 km and an inclination of 72. Six satellites are deployed into six orbit planes. Orbit planes are separated by 24° separation angle. A true anomaly separation in argument of latitude with 52.5° between satellites in adjacent orbit planes is selected too (Wu et al. 2005). Although FORMOSAT-3 is developed with global objectives, comparing the proposed constellations to it provides good insights into the constellations' performance as a baseline. Regional performance of the optimized 2D-LFC, 3D-LFC and FORMOSAT-3/COSMIC is evaluated in terms of COV (λ), the point distribution norm (h) and the number of provided ROEs in the region. Figures 4, 5 and 6 report on the numerical comparison of the three constellations.

Shown in Fig. 5 the 2D-LFC significantly provides more ROEs than the other constellations. This fact is resulted by lower inclination selected for the 2D-LFC which just provides RO to maximum latitude of about 60° (see Fig. 7). On the other hand, the 2D- LFC deploys satellites in lower altitude which not only provides the suitable geometry for

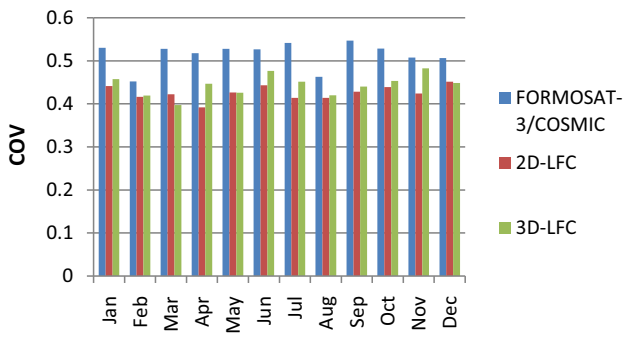

Fig. 4 The regional ROE COVs of the three constellations compared on first days of months in 2013

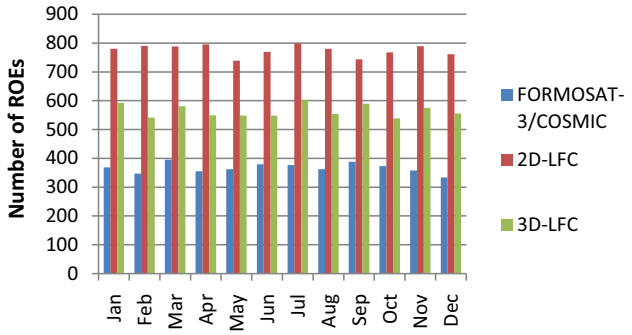

Fig. 5 The number of regional ROEs of the three constellations compared on first day of months in 2013

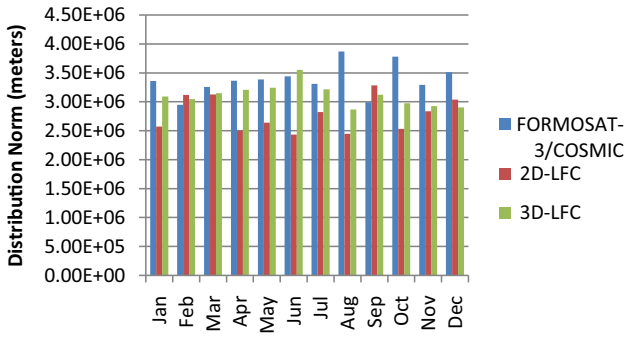

Fig. 6 The regional ROE distribution norms (m) of the three constellations compared on first day of months in 2013

a ROE but also decreases satellites revolution period. The period reduction leads to more pass of satellites over the region and more ROEs. But it should be mentioned that a faster motion of the satellites may cause a reduction in RO observation duration. This fact is investigated by computing the average duration of ROEs on the 12 days for the constellations. These values are 67, 62 and 63 s for FORMOSAT-3, 2D-LFC and 3D-LFC, respectively. According to significant rise of ROEs number, the ROE duration reduction is so small to be ignored. The elliptical orbits deployed by the 3D-LFC are evaluated better than FORMOSAT-3 based on the number of regional ROEs.

Based on numerical results, although the optimization fitness function is based on a volumetric uniformly measure, the optimized constellations enjoy good point-to-point distribution as the COV values demonstrate. According to Fig. 4, the 2D-LFC has the best COV values throughout the year. Moreover, 3D-LFC provides COVs better than FORMOSAT-3 and is also comparable to 2D-LFC, but this evaluation indicates the 2D-LFC's superiority to other constellations again.

Although the 3D-LFC provides proper COVs rather than the other measures, this constellation fails to provide suitable volumetric distribution according to Fig. 6 demonstrating 2D-LFC superiority also to FORMOSAT-3 based on the distribution norm. In other words, the constellation providing

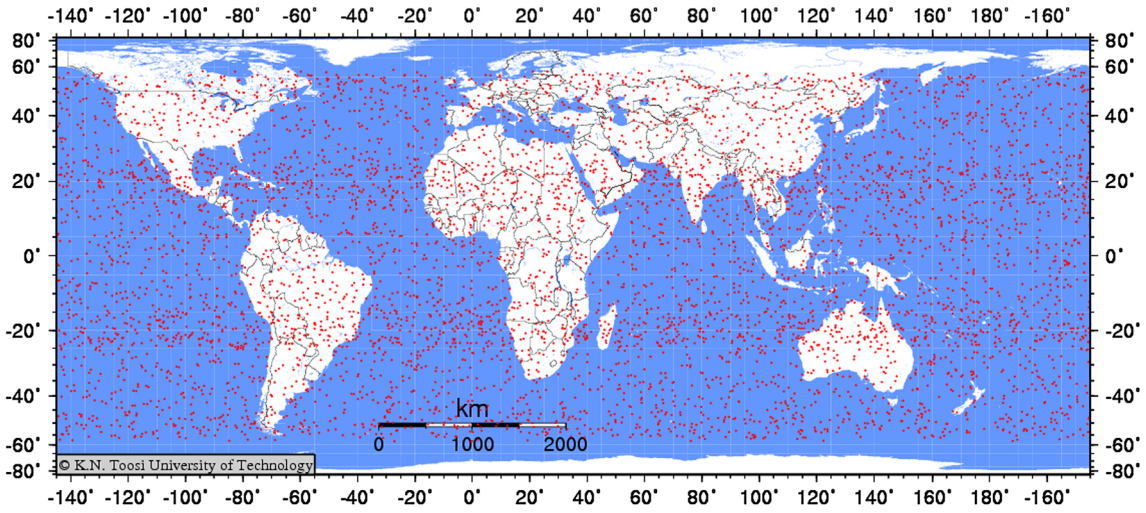

Fig. 7 Global ROEs provided by the optimal 2D-LFC on 1 March 2013

significant number of ROEs with a sufficient enough COVs necessarily covers the region temporally and spatially (i.e., enjoys suitable volumetric distribution). As a result, the 2D-LFC is superior to the others; however, 3D-LFC enjoys better regional performance than FORMOSAT-3. This fact is a proof of the regional optimization approach success. The significant difference between the proposed regional constellations and the globally distributed FORMOSAT-3 can be a good motivation of developing regional RO missions; however, the global coverage is missed. As the results demonstrate, the desired performance in some regions is unreachable by global objectives. This is why six satellites will be deployed to improve regional performance in FORMOSAT-7/COSMIC-2.

RO spatial distribution of the constellations on the worst and best days based on the number of regional ROs is shown in Figs. 8 and 9, respectively. As visually represented, the proposed 2D-LFC provides RO observations for the major number of countries in the region even on the worst day; however, more countries are left without RO observations by FORMOSAT-3/COSMIC.

7.4 Spatial performance variations

It is hard to have an insight into the global performance of an RO mission, especially the temporal distribution, by visual representations (see for e.g. Fig. 7). To have a quantitative study on the performance variation of the optimal 2D-LFC constellation throughout the world, the window representing the study area (Asia Pacific) with dimensions of 48° in latitude and 110° in longitude is slid once along longitude to evaluate longitudinal variations and then along latitude to study latitudinal variations. Distribution norm and number of ROEs are measured and recorded while the window was being moved. Figures 10 and 11 display longitudinal variations and Figs. 12 and 13 show latitudinal performance variations in terms of number of ROEs and the distribution norm, respectively. It should be noted that in these figures the horizontal axes are corresponded to the central point of the window. Also, in Figs. 10 and 11, the constant latitude is 29° and Figs. 12 and 13 shows constant longitude of 80°. The study is carried out on the RO data provided by the optimal 2D-LFC (proposed constellation) on 1 July 2013.

According to the obtained results, there is no significant variation along the longitude. This is clearly resulted by longitudinal uniformity of both constellations' geometry (GPS and the 2D-LFC) relative to the earth. Differently, the performance significantly is a function of latitude. An equatorial symmetry is detected in the performance due the symmetry of the both constellations relative to the equator. Due to this symmetry and also better equatorial coverage of GPS and 2D-LFCs, a significant better performance is expected in equator and the regions close to, while the performance must be poorer as we move toward the polar caps. The performance behavior of the proposed constellation is based on the fact of retaining the good equatorial performance up to the target area which is highlighted by the orange color in the charts. According to Fig. 12, it is seen that number of ROEs decreases as the window distances from equator and again increases by approaching the target area which is optimized by GA. Number of ROEs decreases sharply after crossing Asia Pacific region. As Fig. 13 represents, the distribution norm oscillates in equatorial regions and increases by distancing this regions. It is tried to retain the distribution norm in small values while by crossing the study area the distribution norm increases significantly (as the proposed constellation covers only almost a maximum latitude of the target region represented by Fig. 7). Also, it can be seen that value

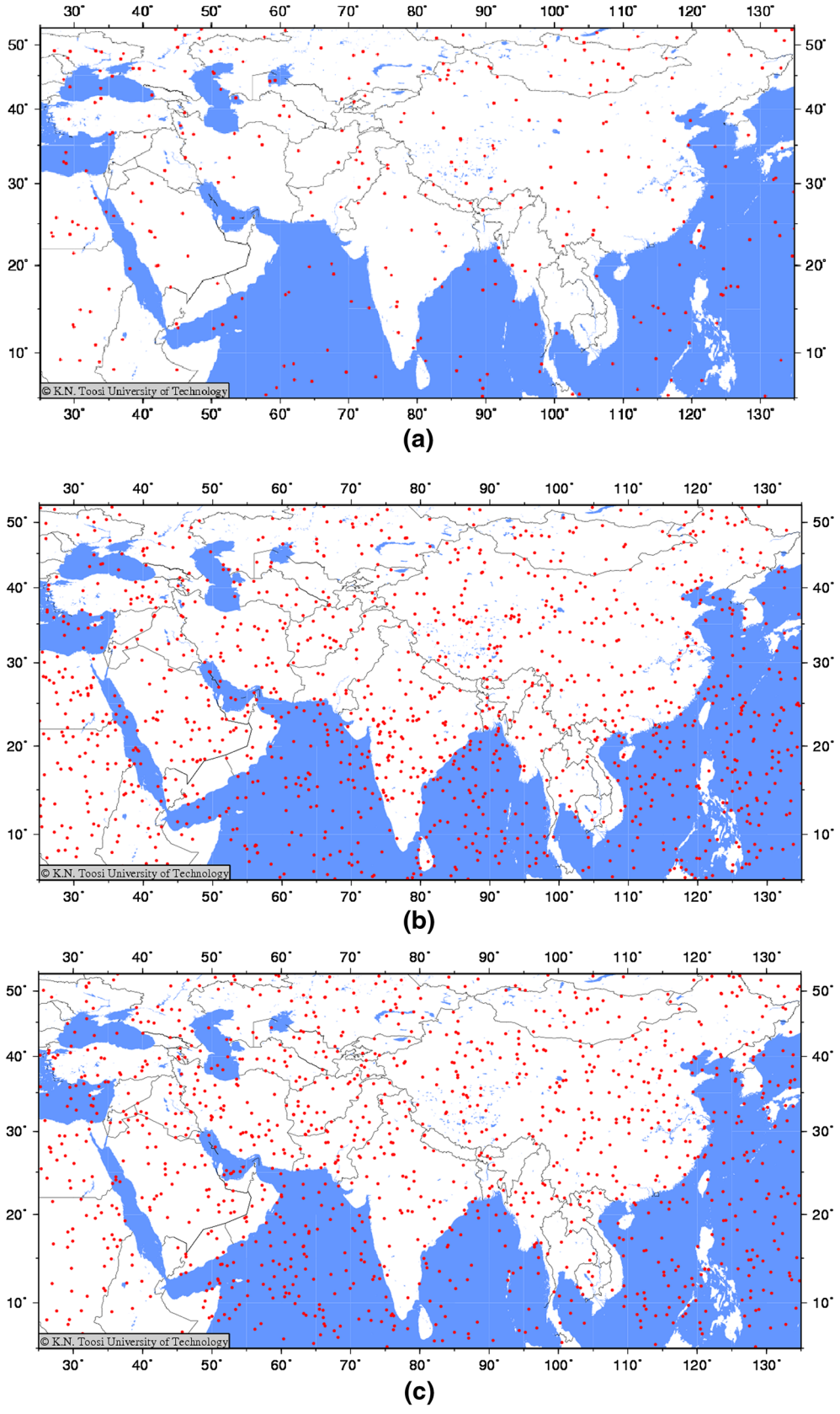

Fig. 8 ROEs in the region on the worst day based on the number of ROEs provided by FORMOSAT-3/COSMIC (**a**), the 2D-LFC (**b**) and the 3D-LFC (**c**)

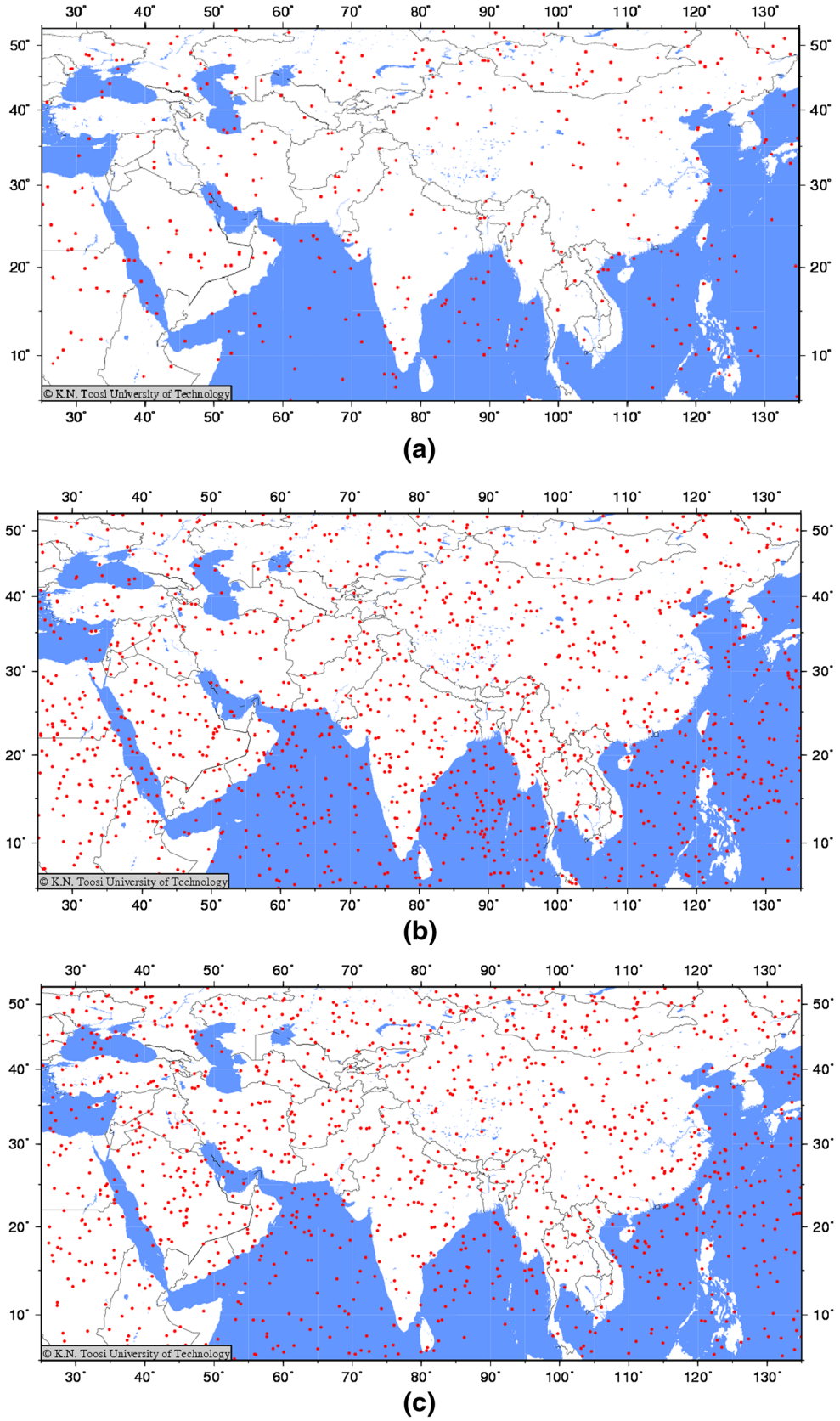

Fig. 9 ROEs in the region on the best day based on the number of ROEs provided by FORMOSAT-3/COSMIC (**a**), the 2D-LFC (**b**) and the 3D-LFC (**c**)

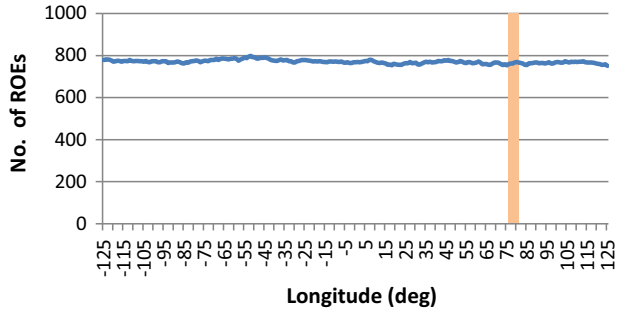

Fig. 10 Longitudinal variations of number of ROEs

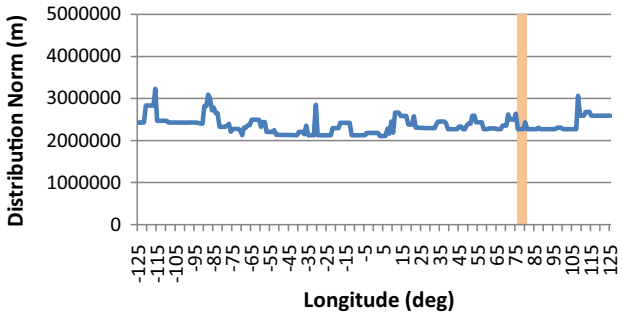

Fig. 11 Longitudinal variations of distribution norm

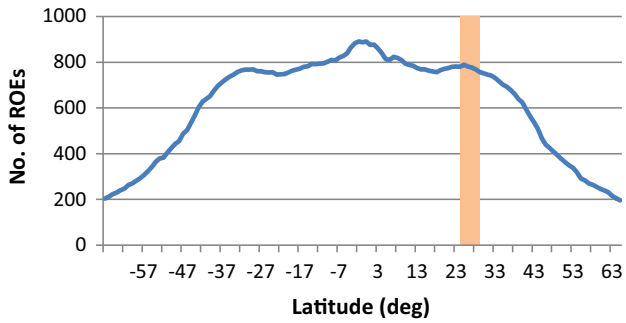

Fig. 12 Latitudinal variations of number of ROEs

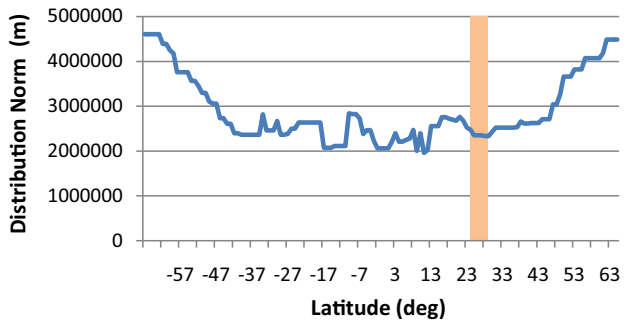

Fig. 13 Latitudinal variations of distribution norm

of the distribution norm in Asia Pacific is slightly larger than some parts of the equatorial regions (the minimum value of the distribution norm).

7.5 Utilizing multiple GNSS

Although GPS is the first, only fully operational GNSS, future generation of RO constellation will be equipped by multi-GNSS receivers due to importance of RO distribution and also to improve quality of RO technique by the increased radio frequencies available for the retrieval processing. Despite sole utilization of GPS by the proposed RO constellation of this research, impact of using multi-GNSS receivers for increasing the number of satellite constellations on the distribution is studied. To this end, GLONASS and Galileo are simulated in addition to GPS. The orbits of Galileo and GLONASS satellites are propagated by the propagation model described in Sect. 7.1 on 1 July 2013. The initial Keplerian elements of these two constellations are extracted from JSatTrak. JSatTrak predicts the position of any satellite in real time, or in the past or future, using advanced SGP4/SDP4 algorithms developed by NASA/NOARD (Hogan and Gaskins 2009).

According to the simulation results, the multi-GNSS receiver usage results in 1612 ROEs in the study area and 11,884 ROEs globally which is significantly larger than the sole use of GPS. Differently, the distribution norm is not improved at all and both cases result in the same value (2.5727e+006 m). This fact can be a proof that only increasing the number of ROEs cannot sufficiently guarantee a suitable distribution; however, the optimization process demonstrated that decreasing value of the distribution norm can result in larger number of ROEs. As a result, increasing the number of satellite constellations to provide RO data improves number of ROEs, but the distribution aspect, i.e., distribution norm, must be considered. However, the application of a multi-GNSS constellation can improve the distribution norm value if the additional GNSS constellations are taken in into account in the optimization process.

7.6 Comparison to traditional methods

Emerging a new atmosphere monitoring system in this region is an alternative to traditional methods. There are more than 800 radiosonde launch sites throughout the world. Nearly all routine radiosonde launches occur 45 min before the official observation time of 00:00 UTC and 12:00 UTC. Small number of launching sites is explained by the relatively large operational cost. Data acquisition by a radiosonde needs already provided ground stations, including the receiving station, the gas supply, the radiosondes, and the personnel in charge which can be highly costly (Douglas 2010). A receiving station costs usually up to $100,000 (U.S. dollars) or at, the lower end, $5000. Each individual radiosonde costs about $200 (Flores et al. 2013). Nevertheless, using the RO data as supplementary or an alternative to radiosonde is strongly suggested.

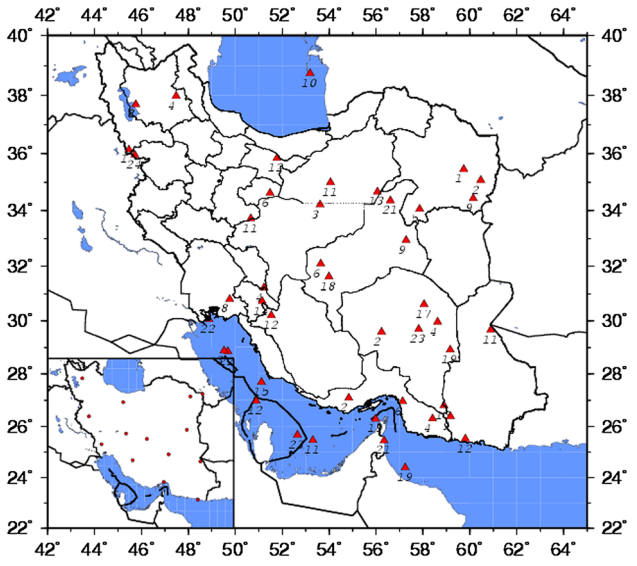

Fig. 14 ROEs in Iran on 1 May 2013 compared to radiosonde launch sites

Iran as a part of international weather and climate society uses 14 sites distributed across the country to launch radiosondes. Supposing the RO observations can provide the same information as a radiosonde, GPS ROEs distribution in Iran is compared to radiosonde sites' distribution. Figure 14 displays the ROEs on 1 May 2013 by the proposed constellation. Moreover, the radiosonde launch sites are shown on the lower left corner. To have a temporal distribution insight, UTC time hour of each ROE is displayed besides.

As Fig. 14 displays, the constellation can provide RO observations in the Caspian Sea, the Persian Gulf, the locations which a radiosonde site establishment in is impossible. It can be a great advantage of developing such system. On the other hand, supposing radiosondes are launched twice a day, there are 28 radiosonde profiles while 45 ROs are observed on the day. Here, in a suitable way, ROEs cover the regions which are left without any launch sites. Moreover, the temporal intervals of ROEs in the dense areas are a proof for a suitable temporal distribution and the success of the devised fitness function in optimization process. As a result, the proposed constellation can be a strong supplementary data acquisition system reducing the traditional meteorological data acquisition costs significantly.

7.7 Orbit maintenance

Once LEO satellites are placed in their mission orbits, mission requirements demand that we maneuver the satellites to correct the orbital elements changed due to perturbing forces. The two important perturbations on LEO satellites, the Earth's oblateness (J_2) and atmospheric drag, may change the proposed constellation elements so that it needs an extra velocity propelling the spacecraft to the desired orbit. In circular orbits such as the proposed constellation and FORMOSAT-3, J_2 causes the right ascension of the ascending node change and the orbit rotates around the Earth. If the satellite is desired to orbit in a repeating ground track, the effect of J_2 must be compensated for which is not the case in this research. But the most important change in orbital elements of the constellations considered here is the altitude decrease due to atmospheric drag. Due to lower satellite altitude of proposed constellation compared to FORMOSAT-3, it is expected that the proposed constellation demands more velocity change to compensate the altitude change. Values of altitude change and needed propelling velocity after 1 year can be approximated (James and Wiley 1999, pp. 144–145). The altitude change is -18.64 and -0.67 km and also the needed compensating velocities are 10.30 and 0.35 m/s for the proposed constellation and FORMOSAT-3, respectively. The proposed constellation needs the spacecrafts to be designed to compensate the altitude change; however, the altitude constraint can be applied if any special hardware or economical limitation is considered in the constellation development.

8 Conclusion

Based on the growing need of better distributed GNSS radio occultation data, we analyzed and designed constellations for GPS radio occultation mission with the optimum performance over the Asia Pacific Region. The genetic algorithm technique constrained to existing constellation pattern theories as frameworks has been used to find the best constellation for the mission. Using Voronoi diagram concept, the distribution norm is used to find the best constellation. This volumetric distribution measure is defined on a 3D space consisting standardized temporal intervals as the third dimension which made a simultaneously temporal and spatial optimization possible. Simulating perturbed orbits instead of Keplerian one led to significantly more accurate pre-analysis. Discussing on the different constellations, the 2D lattice flower constellation is selected to deploy only circular orbits. To maintain symmetry of the satellites' geometry, 3D lattice flower constellation is utilized for the elliptical orbits. The two proposed constellations are compared to existing global radio occultation mission, FORMOSAT-3/COSMIC, in terms of the distribution norm in the space, number of radio occultation events in the region and also COV as a point-to-point distribution measure. The circular orbits patterned by 2D lattice flower constellation are significantly superior to the other constellations by all the terms.

Also the optimal 3D lattice flower constellation enjoys better performance than FORMOSAT-3 demonstrating success of adopted optimization scheme of this paper. By studying the global performance of the optimized 2D-LFC, it is shown that despite longitudinal uniformity of the performance, it is strongly a function of latitude. The obtained variations of evaluation criteria demonstrate that the regional scheme of optimization causes a regional performance almost as suitable as the equatorial regions which enjoy inherent advantages by being located in symmetry axis of satellite constellations. This scheme retains the best performance in equator up to the target latitude; however, the system will be inefficient in vast regions with high latitudes. Hence, it is deduced that the difference between the proposed regional constellations and the globally distributed constellations in terms of regional performance is a good motivation of developing regional RO missions. Impact of using multi-GNSS receivers instead of the sole use of GPS is studied by taking into account the GLONASS and Galileo satellites. Although using multiple GNSS constellations increases number of ROEs, but in some aspects, the distribution is not modified. At last, possibility of using the best proposed constellations as a supplementary or alternative to traditional meteorological data acquisition methods is investigated. Development of such system can strongly decrease cost of data acquisition by radiosondes and support the climate monitoring projects and researches.

References

Abdelkhalik O, Gad A (2011) Optimization of space orbits design for Earth orbiting missions. Acta Astronautica 68:1307–1317. doi:10.1016/j.actaastro.2010.09.029

Anthes R (2011) Exploring Earth's atmosphere with radio occultation: contributions to weather, climate and space weather. Atmos Meas Tech 4:1077–1103

Asvial M, Tafazolli R, Evans BG (2004) Satellite constellation design and radio resource management using genetic algorithm. Communications, IEEE proceedings, pp 151:204–209. doi:10.1049/ip-com:20040291(410)151

Aurenhammer F (1991) Voronoi diagrams—a survey of a fundamental geometric data structure. ACM Comput Sur (CSUR) 23:345–405

Avendaño ME, Davis JJ, Mortari D (2013) The 2-D lattice theory of fower constellations. Celest. Mech. Dyn. Astron. 116:325–337

Bevis M, Businger S, Chiswell S, Herring TA, Anthes RA, Rocken C, Ware RH (1994) GPS meteorology: mapping zenith wet delays onto precipitable water. J Appl Meteorol 33:379–386

Brunini C, Azpilicueta F, Nava B (2013) A technique for routinely updating the ITU-R database using radio occultation electron density profiles. J Geod 87:813–823

Coesa U (1976) Standard atmosphere, 1976. US Government Printing Office, Washington, DC

Cook G (1965) Satellite drag coefficients. Planet Space Sci 13:929–946

Cook K, Fong C-J, Wenkel MJ, Wilczynski P, Yen N, Chang G (2013) FORMOSAT-7/COSMIC-2 GNSS radio occultation constellation mission for global weather monitoring. In: Aerospace conference, 2013 IEEE. IEEE, pp. 1–8

Crossley WA, Williams EA (2000) Simulated annealing and genetic algorithm approaches for discontinuous coverage satellite constellation design. Eng Optim 32:353–371. doi:10.1080/03052150008941304

Davis JJ, Avendaño ME, Mortari D (2013) The 3-D lattice theory of flower constellations. Celest Mech Dyn Astron 116:339–356

Douglas M (2010) Adaptive sounding arrays for tropical regions. In: Extended abstracts, 29th conference on Hurricanes and Tropical Meteorology. Am Meteor Soc Tucson, AZ, pp 12B. 17

Ely T, Crossley W, Williams E (1999) Satellite constellation design for zonal coverage using genetic algorithms. J Astronaut Sci 47:207–228

Flores F, Rondanelli R, Díaz M, Querel R, Mundnich K, Herrera LA, Pola D, Carricajo T (2013) The life cycle of a radiosonde. Bull Am Meteorol Soc 94:187–198

Fong C-J, Shiau W-T, Lin C-T, Kuo T-C, Chu C-H, Yang S-K, Yen NL, Chen S-S, Kuo Y-H, Liou Y-A (2008) Constellation deployment for the FORMOSAT-3/COSMIC mission. IEEE Trans Geosci Remote Sens 46:3367–3379

Fong C-J, Yen NL, Chu C-H, Yang S-K, Shiau W-T, Huang C-Y, Chi S, Chen S-S, Liou Y-A, Kuo Y-H (2009) FORMOSAT-3/COSMIC spacecraft constellation system, mission results, and prospect for follow-on mission. Terrestrial, Atmospheric and Oceanic Sciences 20

Fonseca CM, Fleming PJ (1993) Genetic algorithms for multiobjective optimization: formulation discussion and generalization. In: ICGA, pp 416–423

Goldberg D, Holland J (1988) Genetic algorithms and machine learning. Mach Learn 3:95–99. doi:10.1023/A:1022602019183

Gunzburger M, Burkardt J (2004) Uniformity measures for point sample in hypercubes. Rapp. tech. Florida State University (cf. p 73)

Hogan P, Gaskins T (2009) Spatial information processing: standards-based open source visualization technology. In: AGU fall meeting abstracts, p 04

James RW, Wiley JL (1999) Space mission analysis and design. MicrocosmPress, Torrance

Juang J-C, Tsai Y-F, Chu C-H (2013) On constellation design of multi-GNSS radio occultation mission. Acta Astronaut 82:88–94

Kessler DJ (1990) Collision probability at low altitudes resulting from elliptical orbits. Adv Space Res 10:393–396

Kliore A, Cain DL, Levy GS, Eshleman VR, Fjeldbo G, Drake FD (1965) Occultation experiment: results of the first direct measurement of Mars's atmosphere and ionosphere. Science 149:1243–1248

Le Marshall J, Xiao Y, Norman R, Zhang K, Rea A, Cucurull L, Seecamp R, Steinle P, Puri K, Fu E (2012) The application of radio occultation observations for climate monitoring and numerical weather prediction in the Australian region. Aust Meteorol Oceanogr J 62:323–334

Lee S, Mortari D (2013) 2-D Lattice flower constellations for radio occultation missions. Front Aerosp Eng 2:79–90

Mortari D, Wilkins MP (2008) Flower constellation set theory. Part I: compatibility and phasing. IEEE Trans Aerosp Electron Syst 44:953–962

Mortari D, Wilkins MP, Bruccolerr C (2003) The flower constellations. Adv Astronaut Sci 115:269–290

Mousa A, Aoyama Y, Tsuda T (2006) A simulation analysis to optimize orbits for a tropical GPS radio occultation mission. Earth Planets Space 58:919–925

Poli R, Langdon WB (1998) Schema theory for genetic programming with one-point crossover and point mutation. Evolut Comput 6:231–252

Rider L (1985) Optimized polar orbit constellations for redundant earth coverage. J Astronaut Sci 33:147–161

Rider L (1986) Analytic design of satellite constellations for zonal earth coverage using inclined circular orbits. J Astronaut Sci 34:31–64

Seeber G (2003) Satellite geodesy: foundations, methods, and applications. Walter de Gruyter, Berlin

Speckman L, Lang T, Boyce W (1990) An analysis of the line of sight vector between two satellites in common altitude circular orbits. In: Astrodynamics conference. American Institute of Aeronautics and Astronautics

Walker J (1978) Satellite patterns for continuous multiple whole-Earth coverage. In: Maritime and aeronautical satellite communication and navigation, pp 119–122

Walker JG (1977) Continuous whole-earth coverage by circular-orbit satellite patterns. In: DTIC Document, United Kingdom

Wickert J, Michalak G, Schmidt T, Beyerle G, Cheng C-Z, Healy SB, Heise S, Huang C-Y, Jakowski N, Kohler W (2009) GPS radio occultation: results from CHAMP, GRACE and FORMOSAT-3/COSMIC. Terr Atmos Ocean Sci 20:35

Wilkins MP, Mortari D (2008) Flower constellation set theory part II: secondary paths and equivalency. IEEE Trans Aerosp Electron Syst 44:964–976

Wu B-H, Chu V, Chen P, Ting T (2005) FORMOSAT-3/COSMIC science mission update. GPS Solut 9:111–121

Xu G (2008) Orbits. Springer, Heidelberg

Yan K, Yang F, Pan C, Song J, Ren F, Li J (2013) Genetic algorithm aided gray-APSK constellation optimization. In: Wireless communications and mobile computing conference (IWCMC), 2013 9th international. IEEE, pp 1705–1709

Yunck TP, Chao-Han L, Ware R (2000) A history of GPS sounding. Terr Atmosp Ocean Sci 11:1–20